



ACADEMIC  
PRESS

Available online at [www.sciencedirect.com](http://www.sciencedirect.com)

SCIENCE @ DIRECT®

Journal of Sound and Vibration 269 (2004) 899–912

JOURNAL OF  
SOUND AND  
VIBRATION

[www.elsevier.com/locate/jsvi](http://www.elsevier.com/locate/jsvi)

## Missile flutter experiment and data analysis using wavelet transform

Kaiping Yu<sup>a,\*</sup>, Jiyuan Ye<sup>a</sup>, Jingxiang Zou<sup>a</sup>, Bingyuan Yang<sup>b</sup>, Hua Yang<sup>b</sup>

<sup>a</sup> *Department of Astronautics and Mechanics, Harbin Institute of Technology, Harbin 150001, China*

<sup>b</sup> *The No 8 Design and Research Institute of Shanghai Academy of Spaceflight Technology, Shanghai 200233, China*

Received 5 March 2002; accepted 9 January 2003

---

### Abstract

A modal parameter identification method of impulse response function, based on a modulated Gaussian wavelet transform, is presented. The factors influencing the identification accuracy and the required conditions of using this parameter identification method are discussed. Numerical verification of the proposed method is presented for several two-degree-of-freedom examples. A wind tunnel flutter experiment on a wing model of missiles is introduced. The data set from the flutter test is analyzed by using the proposed wavelet transform method. The first two order modal parameters of the wing model are identified, and then the critical dynamic stress is predicted by using the flutter stability parameter method. Finally, the results are compared with the results of FFT analysis.

© 2003 Elsevier Ltd. All rights reserved.

---

### 1. Introduction

The flutter analysis of missiles is mainly concerned with the flutter of wings for the anti-aircraft missiles. Because the stiffness of control systems of wings is relatively small, the first two order modes of wings are mainly warping and torsion, and their coupling may cause flutter easily. Moreover, there are many factors that would influence the flutter, and many hypotheses are required for the analysis, and thus the reliability of conclusion is limited. Therefore, it is important to verify the conclusion through experiments. At present, the experimental method on the design of missiles is mainly the wind tunnel flutter experiment. The flutter critical point is predicted through modal parameter identification based on the modal structure under the sub-critical state. The common way is to get the freedom decrement signal or impulse response of the structure

---

\*Corresponding author.

*E-mail addresses:* [yukp@hope.hit.edu.cn](mailto:yukp@hope.hit.edu.cn), [yejiyuan@yahoo.com.cn](mailto:yejiyuan@yahoo.com.cn) (K. Yu).

through the random decrement technique, and then get modal parameters through the regular methods, such as the least-squares iteration method, ITD method and the complex exponential method [1]. However, these methods are sensitive to the noise. In recent years, many scientists [2–5] presented the theory of using the wavelet transform method for identifying the modal parameters of a structural system. Staszewski and Cooper [2] have used this method in an analysis of the flutter experimental data of planes. Lamarque et al. [5] have used this method in an analysis of the vibration experimental data of bridges. However, this method has yet not been used in analysis of the wind tunnel flutter experimental data of wings.

In this paper, the modal parameter identification method based on the modulated Gaussian wavelet is introduced and analyzed. And then the flutter experiment on the wing of the anti-aircraft missile is also introduced. The wavelet transform method based on the modulated Gaussian wavelet and the frequent response analysis are used in identifying the experimental data, respectively. According to the modal parameters that are identified, the critical dynamic pressure is determined. Finally, the results of these two methods are compared.

## 2. The general Morlet wavelet

The general form of Morlet wavelet is [1]

$$g(t) = \pi^{-1/4}(e^{i\omega_0 t} - e^{-\omega_0^2/2})e^{-t^2/2}. \tag{1}$$

In this paper, the generalized Morlet wavelet can be written as

$$g(t) = c(e^{i\omega_0 t} - e^{-\omega_0^2\sigma^2/2})e^{-t^2/(2\sigma^2)}, \tag{2}$$

where  $c$  is a non-zero constant,  $\omega_0$  is the modulated frequency,  $\sigma$  is the Gauss parameter.  $g(t)$  is also called as Morlet wavelet with an adjustable parameter. Its Fourier transform can be written as

$$\hat{g}(\omega) = c\sigma\sqrt{2\pi}[e^{-\sigma^2(\omega-\omega_0)^2/2} - e^{-\sigma^2(\omega^2+\omega_0^2)/2}]. \tag{3}$$

It is a non-orthogonal, redundant wavelet. Usually, we need  $\sigma\omega_0 > 5$  so that we can improve the accuracy of the analysis by reducing the redundancy. It can be easily verified that this wavelet has some characteristics as follows:

$$\int_{-\infty}^{+\infty} g(t) dt = \hat{g}(0) = 0, \tag{4}$$

$$\int_{-\infty}^{+\infty} |g(t)|^2 dt = \frac{\sigma\sqrt{\pi}}{c^2}(1 + e^{-\omega_0^2\sigma^2} - 2e^{-3\omega_0^2\sigma^2/4}) < +\infty, \tag{5}$$

$$\int_{-\infty}^{+\infty} t|g(t)|^2 dt = 0. \tag{6}$$

Usually, we employ  $c = 1$ , and we often ignore the second term in the bracket of Eqs. (1) and (2) because they are much less than the first term when  $\sigma\omega_0 > 5$ . Thus, its wavelet base function

and Fourier transform are given by

$$g_{a,b}(t) = g\left(\frac{t-b}{a}\right) = e^{i\omega_0 t - b/a} e^{-(t-b/a)^2 / (2\sigma^2)}, \tag{7}$$

$$\hat{g}_{a,b}(\omega) = \sqrt{a} \hat{g}(a\omega) e^{-i\omega b} = \sigma \sqrt{2a\pi} e^{-\sigma^2(a\omega - \omega_0)^2 / 2} e^{-i\omega b}, \tag{8}$$

where  $a$  is the frequency scale parameter and  $b$  is the time location parameter. Its time–frequency window is

$$[b - a \Delta g \sqrt{\sigma}, b + a \Delta g \sqrt{\sigma}] \times \left[ \frac{\omega_0}{a} - \frac{\Delta \hat{g}}{a \sqrt{\sigma}}, \frac{\omega_0}{a} + \frac{\Delta \hat{g}}{a \sqrt{\sigma}} \right], \tag{9}$$

where  $\Delta g$ ,  $\Delta \hat{g}$  are the radii of time and frequency window of the modulated frequency Gauss mother wavelet, respectively. It can be seen that this wavelet base function can automatically adjust the time–frequency resolution with changing frequency parameters. Once the center of the frequency window is fixed, the width of the window, as well as the time–frequency resolution of this wavelet, can be adjusted by choosing the Gauss parameter. When  $\sigma = 1$ , the studied wavelet becomes the Morlet wavelet, and it also has good band-pass characters. As presented in Ref. [2], when the wavelet transform method is used to identify the modal parameters of a structural system, its accuracy is closely related to the time–frequency resolution of the wavelet. For this reason, in this paper we use the Morlet wavelet with an adjustable parameter.

### 3. Identification of a modal parameter

#### 3.1. System of single degree of freedom (s.d.o.f.)

The impulse response function of a structural system contains its natural characters. An impulse response function of an s.d.o.f. system can be written as

$$h(t) = A e^{-\zeta \omega_n t} \sin(\omega_d t + \phi_0). \tag{10}$$

Its wavelet transform is

$$\begin{aligned} WT_h(a, b) &= \langle h, g_{a,b} \rangle = \frac{1}{2\pi} \langle \hat{h}, \hat{g}_{a,b} \rangle = \frac{1}{2\pi} \int_{-\infty}^{+\infty} \hat{h}(\omega) \hat{g}_{a,b}^*(\omega) d\omega \\ &= \frac{\sqrt{a}}{2\pi} \int_{-\infty}^{+\infty} \hat{h}(\omega) \hat{g}(a\omega) e^{i\omega b} d\omega \\ &= A \frac{\sqrt{a}}{2\pi} \int_{-\infty}^{+\infty} \frac{1}{\omega_n^2 - \omega^2 + 2i\zeta\omega_n\omega} \hat{g}(a\omega) e^{i(\omega b + \phi_0)} d\omega. \end{aligned} \tag{11}$$

In Eq. (11), we define that  $z = i\omega$  and then use the residue theorem

$$\begin{aligned} WT_h(a, b) &= A \frac{\sqrt{a}}{2i} e^{-\zeta \omega_n b + \phi_0} (\hat{g}(a\zeta\omega_n i + a\omega_d) e^{i(\omega_d b + \phi_0)} \\ &\quad - \hat{g}(a\zeta\omega_n i - a\omega_d) e^{-i(\omega_d b - \phi_0)}) \\ &= (A_1 e^{(\omega_d b + \phi_1)i} - A_2 e^{(-\omega_d b + \phi_2)i}) e^{-\zeta \omega_n b + \phi_0}, \end{aligned} \tag{12}$$

where

$$\begin{aligned}
 A_1 &= A\sigma\sqrt{a\pi/2}e^{-\sigma^2(a\omega_d-\omega_0)^2/2+(\sigma a\xi\omega_n)^2/2}, \\
 A_2 &= A\sigma\sqrt{a\pi/2}e^{-\sigma^2(a\omega_d+\omega_0)^2/2+(\sigma a\xi\omega_n)^2/2}, \\
 \phi_1 &= -a\xi\omega_n\sigma^2(a\omega_d-\omega_0)-\pi/2, \\
 \phi_2 &= a\xi\omega_n\sigma^2(a\omega_d+\omega_0)-\pi/2.
 \end{aligned}
 \tag{13}$$

$A_2$  can also be written as

$$A_2 = A\sigma\sqrt{a\pi/2}e^{-\sigma^2[(a\omega_n\sqrt{1-2\xi^2}+\omega_0)^2+2a\omega_0\omega_n(\sqrt{1-\xi^2}-\sqrt{1-2\xi^2})]/2}.
 \tag{14}$$

From Eq. (14), we can see that, because  $\sqrt{1-\xi^2}-\sqrt{1-2\xi^2} > 0$ ,  $A_2$  is almost equal to zero and hence can be neglected. Thus, we can derive from Eq. (12) that

$$|WT_h(a, b)| = A_1 e^{-\xi\omega_n b + \phi_0},
 \tag{15}$$

$$\angle WT_h(a, b) = \omega_d b + \phi_1.
 \tag{16}$$

A logarithm of the module and the phase of the wavelet transform become linear functions of the time parameter  $b$ . They are shown as two lines with the scale of a half logarithm. We can get the modal frequency and modal damping from the slopes of these two lines. For a s.d.o.f. problem, this method has a high accuracy of identification.

### 3.2. System of m.d.o.f.

The impulse response in one point can be expressed as the superposition of the  $N$  most relevant modes of the structure:

$$h(t) = \sum_{j=1}^N h_j(t) = \sum_{j=1}^N A_j e^{-\xi_j\omega_{nj}t} \sin(\omega_{dj}t + \phi_{0j}),
 \tag{17}$$

where  $A_j$  is the residue magnitude,  $\xi_j$  is the modal damping ratio,  $\omega_{nj}$  is the undamped angular frequency,  $\omega_{dj}$  is the damped angular frequency and  $\phi_{0j}$  is the initial phase of the  $j$ th mode. From Eqs. (12)–(14), we can define a linear transformation as  $WT$ . The  $WT$  of  $h(t)$  in Eq. (17) is

$$\begin{aligned}
 WT_h(a, b) &= \sum_{j=1}^N WT_{h_j}(a, b) \\
 &\cong \sum_{j=1}^N A_j \sqrt{a} e^{-\sigma^2(a\omega_{dj}-\omega_0)^2/2+(\sigma a\xi_j\omega_{nj})^2/2} e^{-\xi_j\omega_{nj}b+\phi_{0j}} e^{(\omega_{dj}b+\phi_j)i} \\
 &= \sum_{j=1}^N A_j \sqrt{a} \lambda_j e^{-\xi_j\omega_{nj}b+\phi_{0j}} e^{(\omega_{dj}b+\phi_j)i}.
 \end{aligned}
 \tag{18}$$

If the center of frequency window of the wavelet base is approximately equal to one of the  $N$  modal frequencies, and the corresponding mode gives the main contribution to the sum of the terms in Eq. (18), the modal filter can be realized. For this purpose, we study the coefficients of the Eq. (18). At first,  $\lambda_j$  is given by

$$\begin{aligned} \lambda_j &= e^{-\sigma^2(a\omega_{dj}-\omega_0)^2+(\sigma a\xi_j\omega_{nj})^2/2} \\ &= e^{-(\sigma^2/2)(a\omega_{nj}\sqrt{1-2\xi_j^2}-\omega_0\sqrt{1-\xi_j^2}/\sqrt{1-2\xi_j^2})^2+(\sigma^2/2)\omega_0^2\xi_j^2/(1-2\xi_j^2)}. \end{aligned} \tag{19}$$

$\lambda_j$  will get to its maximum when

$$\begin{aligned} a &= a_j = \omega_0\sqrt{1-\xi_j^2}/(\omega_{nj}(1-2\xi_j^2)) \\ &= \frac{\omega_0}{\omega_{nj}}\left(1 + \frac{3}{2}\xi_j^2 + \frac{23}{8}\xi_j^4 + A\right) \cong \frac{\omega_0}{\omega_{nj}}, \end{aligned} \tag{20}$$

and at this time  $\omega_0/a$  (center of frequency window of the wavelet base) is approximately equal to the  $j$ th modal frequency  $\omega_{nj}$ . If  $A_j$  of the corresponding mode is at the same level as the other modes, we can say that this mode gives the main contribution to the sum in Eq. (18). Eq. (18) can be rewritten as

$$WT_h(a_j, b) \cong A_j\lambda_j\sqrt{a_j}e^{-\xi_j\omega_{nj}b+\phi_{0j}}e^{(\omega_{dj}b+\phi_j)i}. \tag{21}$$

Thus, this multi-degree-of-freedom system is decoupled; then we can identify the modal parameters through Eqs. (15) and (16).

#### 4. Analysis of the method

From the last section, we can see that the generalized Morlet wavelet’s capability of decoupling is closely related to the character of its band-pass filter. And the identificational errors are mainly coming from the mode which the wavelet cannot completely filter. To discuss this problem, we consider the most adjacent two modes of the m.d.o.f. as a two-degree-of-freedom system, for example, the  $j$ th and  $(j+1)$ th modes. Thus, Eq. (18) is rewritten as

$$\begin{aligned} WT_h(a_j, b) &\cong A_j\lambda_j\sqrt{a_j}e^{-\xi_j\omega_{nj}b+\phi_{0j}}e^{(\omega_{dj}b+\phi_j)i} \\ &\quad + A_{j+1}\lambda_{j+1}\sqrt{a_{j+1}}e^{-\xi_{j+1}\omega_{nj+1}b+\phi_{0j+1}}e^{(\omega_{dj+1}b+\phi_{j+1})i}. \end{aligned} \tag{22}$$

Obviously, if  $A_j \gg A_{j+1}$ , it is easy to filter the lower mode, but it is probably difficult to filter the higher one and vice versa. Thus, we consider this problem on the basis that  $A_j$  and  $A_{j+1}$  are at the same level. To make the analysis convenient, we let  $j=1$  and  $j+1=2$ , and define the influence factor as

$$\gamma_j = -\sigma^2(a_j\omega_{dj} - \omega_0)^2/2 + \sigma^2(a_j\xi_j\omega_{nj})^2/2, \quad j = 1, 2. \tag{23}$$

In practice, we can use the finite element method or other methods of modal parameter identification to get the natural frequency of the system accurately. So we usually make

$$a = a_j = \omega_0/\omega_{nj}, \quad j = 1, 2. \tag{24}$$

When  $a = a_1 = \omega_0/\omega_{n1}$ , there are

$$\begin{aligned} \gamma_1 &= -\sigma^2 \omega_0^2 \left( 1 - \xi_1^2 - \sqrt{1 - \xi_1^2} \right), \\ \gamma_2 &= -\sigma^2 \omega_0^2 \left[ \frac{\omega_{n2}^2}{\omega_{n1}^2} (1 - 2\xi_1^2) - 2 \frac{\omega_{n2}}{\omega_{n1}} \sqrt{1 - \xi_1^2} + 1 \right] / 2. \end{aligned} \tag{25}$$

Usually, it is the influence factor of the higher mode that affects the accuracy of low modal identification. It is easy to verify that  $\gamma_1 > 0$ . If at the same time  $\gamma_2 > 0$ , we would think that it is impossible that  $\lambda_j \gg \lambda_{j+1}$ . In other words, it is difficult for the wavelet to achieve the modal filter. Otherwise, the possibility of realization of the modal filter will greatly increase. For this reason, we can use  $\gamma_2 < 0$  as a necessary condition for filtering the low mode. For this goal, there must be

$$\frac{\omega_{n2}^2}{\omega_{n1}^2} (1 - 2\xi_1^2) - 2 \frac{\omega_{n2}}{\omega_{n1}} \sqrt{1 - \xi_1^2} + 1 > 0 \tag{26}$$

or

$$\frac{\omega_{n2}}{\omega_{n1}} > \frac{\sqrt{1 - \xi_1^2} + \xi_1}{1 - 2\xi_1^2}. \tag{27}$$

Likewise, when  $a = a_2 = \omega_0/\omega_{n2}$ , usually it is the influence factor of the lower mode that affects the accuracy of the high modal identification. In this case, there are

$$\begin{aligned} \gamma_1 &= -\sigma^2 \omega_0^2 \left[ \frac{\omega_{n1}^2}{\omega_{n2}^2} (1 - 2\xi_2^2) - 2 \frac{\omega_{n1}}{\omega_{n2}} \sqrt{1 - \xi_2^2} + 1 \right] / 2, \\ \gamma_2 &= -\sigma^2 \omega_0^2 \left( 1 - \xi_2^2 - \sqrt{1 - \xi_2^2} \right). \end{aligned} \tag{28}$$

Obviously,  $\gamma_2 > 0$ , and in this case the required condition for the wavelet transform method to filter the high mode is  $\gamma_1 < 0$ . There must also be that

$$\frac{\omega_{n1}^2}{\omega_{n2}^2} (1 - 2\xi_2^2) - 2 \frac{\omega_{n1}}{\omega_{n2}} \sqrt{1 - \xi_2^2} + 1 > 0 \tag{29}$$

or

$$\frac{\omega_{n1}}{\omega_{n2}} < \frac{\sqrt{1 - \xi_2^2} - \xi_2}{1 - 2\xi_2^2}. \tag{30}$$

We can conclude that

- (i) When the frequency parameter is approximately equal to the modal frequency to be identified, the necessary conditions for the wavelet transform method to filter the adjacent two modes simultaneously are given by Eqs. (27) and (30). We can rewrite them as

$$\frac{\omega_{n2}}{\omega_{n1}} > \max \left\{ \frac{\sqrt{1 - \xi_1^2} + \xi_1}{1 - 2\xi_1^2}, \frac{1 - 2\xi_2^2}{\sqrt{1 - \xi_2^2} - \xi_2} \right\}. \tag{31}$$

For example, we consider a structural system that the damping of its materials is supposed to be a small proportional damping. This means that its value is in the range [0.001 0.1]. If the ratio of the two modal frequencies to be identified is less than 1.12 (the corresponding two modal damping ratios are 0.1), the Morlet wavelet transform method should not be used. If the ratio is more than 1.12, however, we can use this method. The identification accuracy for the cases of large damping is lower than that for the cases of small damping. In other words, from Eq. (31), we know that this method is applicable except for the cases of large damping and close modal frequencies.

- (ii) Usually,  $\omega_0$  is more than 5, and in most earlier papers which use the Morlet wavelet transform method, the authors make  $\omega_0 = 2\pi$ . However, according to the studies in this paper, if the condition of Eq. (31) is satisfied, we can conclude that the identification accuracy can be largely improved by increasing the value of  $\omega_0$  based on Eqs. (25) and (28). From Eqs. (9) and (24), we can see that the value of frequency parameter  $a$  increases with  $\omega_0$ . Thus, the frequency window becomes more narrow, and the time window becomes wider. These make the frequency resolution to increase, and thus the accuracy to improve. Nevertheless, the improvement of accuracy is restricted by the uncertainty principle. If the resolution of time is too low, the total accuracy of the wavelet transform would be impaired, even the transformation itself would be senseless.
- (iii) After  $\omega_0$  is defined, the center of frequency window of the wavelet is definite. The generalized Morlet wavelet transform method in this paper can be improved by adjusting the Gauss parameter  $\sigma$ . However, because it only adjusts the width of the window, the change of the value of  $\sigma$  should be restricted.
- (iv) The purpose of adjusting the values of  $\omega_0$  and  $\sigma$  is to make the difference between the identified value of natural frequency and the known one as little as possible. So the identified value is equal to the damping ratio.

## 5. Numerical example

To verify the conclusions of this paper, and to analyze the numerical character of the wavelet transform method for modal parameter identification, in this section we consider the following two examples. In the first one, the difference between the adjacent modal frequencies is rather great, but in the other one, it is small. The influence of different damping and Gauss parameter  $\sigma$  is included in the study of the first example. And when we study the second one, the influence of the two approximately equivalent modal frequencies and the modulated frequency parameter  $\omega_0$  is included. In the process of simulation, we add Gaussian white noise to the impulse response function of the system. We also define the signal-to-noise ratio as the specific value of the standard difference of the original signal ( $y_0$ ) to the standard difference of the data that include the noise signal ( $y$ ):

$$SNR = \frac{std(y_0)}{std(y - y_0)}. \quad (32)$$

Table 1  
Natural frequencies and damping ratio estimation results from Example 1

| Example 1               |                | Estimated frequency (Hz) | Error ( ) | Estimated damping ratio | Error ( ) |
|-------------------------|----------------|--------------------------|-----------|-------------------------|-----------|
| Low damping ratio with  | $\sigma = 1$   | 9.98136                  | 1.86411   | 0.07959                 | 0.50777   |
|                         |                | 30.16679                 | 0.55597   | 0.04178                 | 4.47321   |
| High damping ratio with | $\sigma = 1$   | 10.31912                 | 3.19124   | 0.32445                 | 18.85641  |
|                         |                | 27.57614                 | 8.07952   | 0.08938                 | 10.61993  |
|                         | $\sigma = 1.1$ | 10.20106                 | 2.01062   | 0.37167                 | 7.08251   |
|                         |                | 28.94067                 | 3.53117   | 0.09179                 | 8.21364   |

Table 2  
Natural frequencies and damping ratio estimation results of Example 2

| Example 2         | Frequency (Hz) | SNR | Estimated frequency (Hz) | Error ( ) | Estimated damping ratio | Error ( ) |
|-------------------|----------------|-----|--------------------------|-----------|-------------------------|-----------|
| $\omega_0 = 2\pi$ | 25             | 100 | 24.98126                 | 0.07496   | 0.05693                 | 3.50909   |
|                   |                | 20  | 25.13172                 | 0.52688   | 0.05421                 | 4.47321   |
|                   |                | 5   | 25.51015                 | 2.04062   | 0.05176                 | 5.89091   |
|                   | 30             | 100 | 30.03817                 | 0.12723   | 0.02004                 | 0.20913   |
|                   |                | 20  | 30.04681                 | 0.15603   | 0.01939                 | 3.05215   |
|                   |                | 5   | 30.07074                 | 0.23581   | 0.01916                 | 4.21354   |
| $\omega_0 = 6\pi$ | 27             | 100 | 27.09737                 | 0.36063   | 0.05736                 | 4.29091   |
|                   |                | 20  | 27.12223                 | 0.45271   | 0.05816                 | 5.74509   |
|                   |                | 100 | 29.91433                 | 0.28557   | 0.01802                 | 9.90000   |
|                   | 30             | 20  | 29.88824                 | 0.37253   | 0.01610                 | 19.47327  |
|                   |                | 100 | 27.96961                 | 6.76834   | 0.02688                 | 51.1158   |
|                   |                | 30  | 29.35183                 | 2.16057   | 0.02547                 | 27.37165  |

The error of identification is

$$\text{error} = \left| \frac{\text{value from theory} - \text{estimated}}{\text{value from theory}} \right|.$$

**Example 1.** The theoretical values of the two modal frequencies are  $f_1 = 10$  Hz,  $f_2 = 30$  Hz. With the condition  $\omega_0 = 2\pi$ , we consider two sets of damping values. One is the case of low damping ratio in which  $\xi_1 = 0.08$ ,  $\xi_2 = 0.04$ , and the other is the case of high damping ratio in which  $\xi_1 = 0.4$ ,  $\xi_2 = 0.1$ . SNR of the data is 100. In the case of the high damping ratio, We make  $\sigma = 1$  and 1.1, respectively, to study the influence of  $\sigma$ . The results of identification and the error are shown in Table 1. It is shown that the identification accuracy for the problem of large damping is acceptable, even though it is relatively low. And it can be improved by adjusting the Gauss parameter.

**Example 2.** The theoretical values of the two modal damping ratio are  $\xi_1 = 0.055$  and  $\xi_2 = 0.02$ . The first modal frequency is 25, 27, 29 Hz. And the second modal frequency is  $f_2 = 30$  Hz. The results of identification are shown in Table 2, Figs. 1 and 2, with the condition of  $\sigma = 1$  and  $\omega_0 = 2\pi, 4\pi$ , respectively.



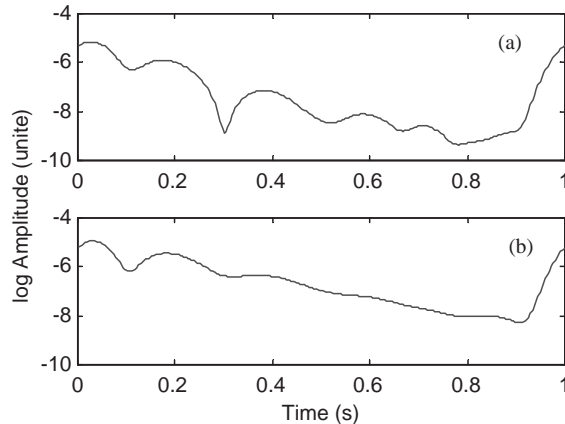


Fig. 1. Semi-logarithmic plot of the module of the wavelet transform of impulse response function ( $\omega_0 = 2\pi$ ,  $SNR=20$ ): (a) first mode, 25 Hz and (b) second mode, 30 Hz.

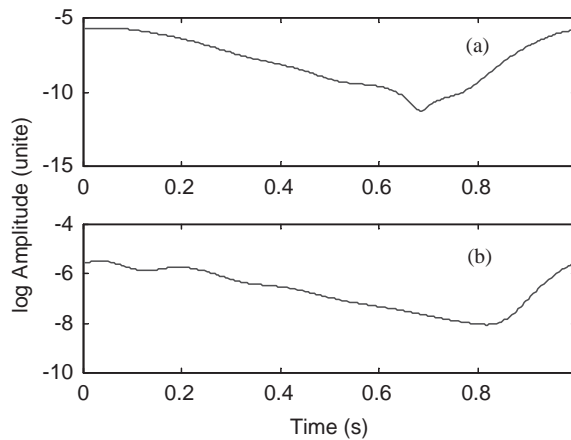


Fig. 2. Semi-logarithmic plot of the module of the wavelet transform of impulse response function ( $\omega_0 = 4\pi$ ,  $SNR=20$ ): (a) first mode, 25 Hz; (b) second mode, 30 Hz.

Figs. 1 and 2 are a semi-logarithmic plot of the module of the wavelet transform of impulse response function, where the first modal frequency is 25, and  $SNR=20$ .

It can be seen that in Fig. 1, the middle part of the curves cannot be regressed to appropriate lines. So it is difficult to get the slope of the lines. Thus, the results of identification are not given for this case.

On the contrary, the curves in Fig. 2 can be easily identified. The results of identification are shown in Table 2. All of the  $\omega_0$  used in this example can help to get a comparatively high accuracy of identification. It is illustrated that the selection of  $\omega_0$  has great influence on the accuracy. In this example, we use 27 and 29 Hz as the first modal frequency. It can be seen that the accuracy of the wavelet transform method is impaired with the approaching of the two adjacent modal

frequencies. For this example, when the two frequencies are 27 and 30 Hz, respectively, the results of identification are acceptable. It shows that this method can be used for identifying the problem in which the difference between two adjacent modes is little. But when the two frequency are 29 and 30 Hz, the results are unacceptable. At this time, the ratio of the high modal frequency to the low one is not satisfied with Eq. (31). So the wavelet transform method is not applicable according to the conclusion of the forth section.

Also in Table 2 we did not list the results in the cases of  $SNR = 5$  and  $5, 20$  when  $\omega_0 = 6\pi$  and  $\omega_0 = 14\pi$ , respectively. The reason is under such cases, there are such big errors in the results that it is nonsensical to list such results.

## 6. The wind tunnel flutter experiment on wing model of missile

In the wind tunnel experiment, because of the limitation of band of the airflow noise, the structural response is too faint to be analyzed. For this reason, we install an exciter on the experimental structure and give a random excitation to the wing surface to increase the bandwidth. The excitation location is shown in Fig. 3. The random excitation comprises the magnetic exciter and power amplifier. The white-noise signal is generated by the dynamic signal analyzer.

The measuring system can be seen in Fig. 4. In this paper, the signal to be analyzed is sampled by BK4343 transducer.

We gradually increase the wind tunnel dynamic pressure from the low dynamic pressure under which the flutter is impossible to the point at which the flutter happens. One set of the original experimental data can be seen in Table 3.

The sampling frequency is 500 Hz, and the length of the record is about 25 s.

## 7. The disposal and analysis of the experimental data

At first, we analyze the power spectrum density (PSD) of the experimental data (see Fig. 5a).

From Fig. 5a we can see that there is a relatively large disturbance at the low frequency. Here the data are obtained from the second data set in Table 3 and in next figures. Before the analysis,

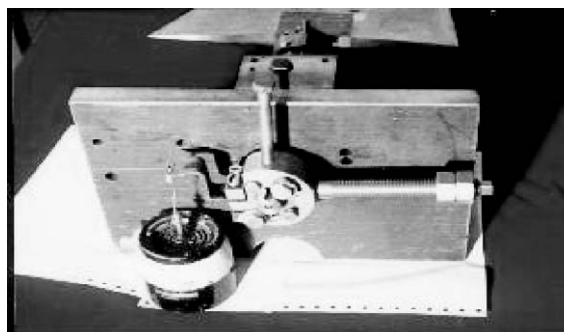


Fig. 3. The exciting location.

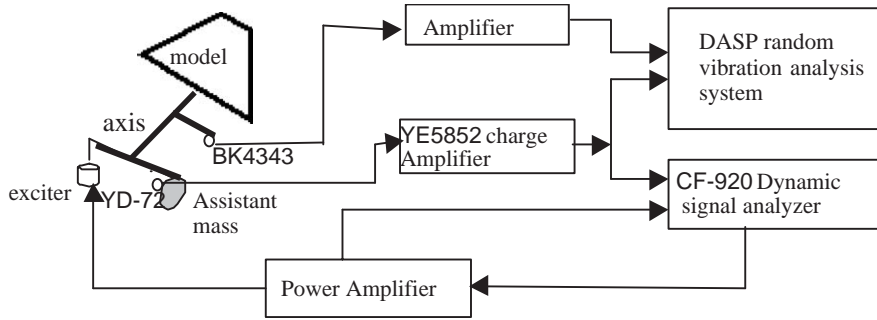


Fig. 4. Measuring system.

Table 3  
Original experimental data

| Order number | Angle of wing model | Modal frequency of the ground (Hz) |              | Parameter of the wind tunnel |                                |
|--------------|---------------------|------------------------------------|--------------|------------------------------|--------------------------------|
|              |                     | First order                        | Second order | Mach number                  | Airflow dynamic pressure (kPa) |
| 1            | 2°42'               | 26.5                               | 47.0         | 1.53                         | 63.92                          |
| 2            |                     |                                    |              |                              | 66.91                          |
| 3            |                     |                                    |              |                              | 71.27                          |
| 4            |                     |                                    |              |                              | 97.9                           |
| 5            |                     |                                    |              |                              | 96.23                          |

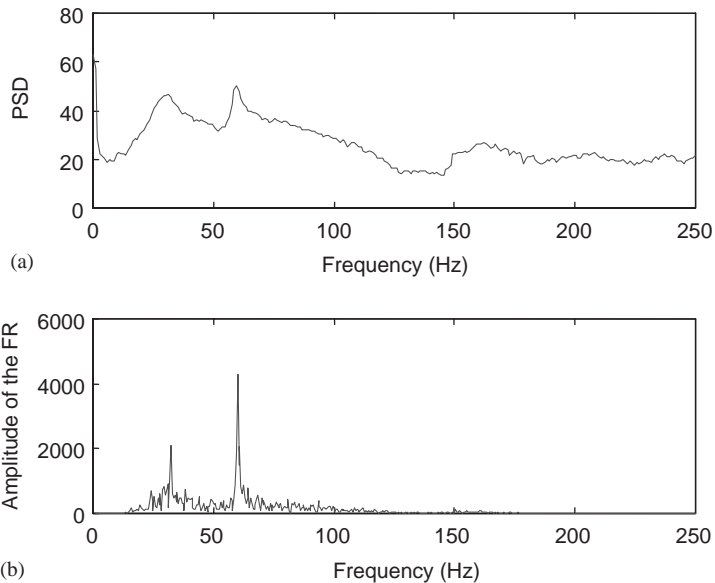


Fig. 5. Frequency response plot of the experimental data: (a) estimated from the original data and (b) obtained by random decrement technique.

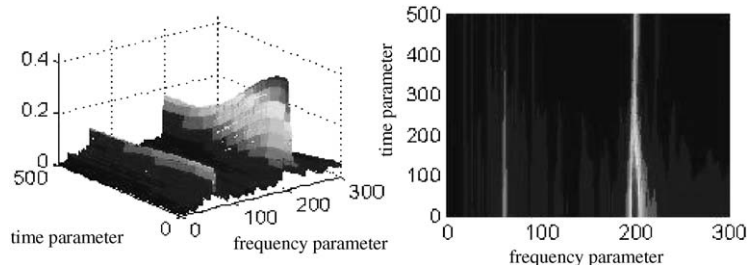


Fig. 6. Three-dimensional time–frequency plot of the wavelet transform of the experimental data (a) and its projection (b).

Table 4

Results of modal parameter identification and estimation of flutter critical dynamic pressure

| Order number | Modal parameters through Fourier analysis |                                       |                                       |  | Modal parameters through wavelet analysis |                                       |                                       |  | Critical dynamic pressure predicted |                        |
|--------------|---|---------------------------------------|---------------------------------------|--|---|---------------------------------------|---------------------------------------|--|-------------------------------------|------------------------|
|              | First order frequency ( $f_1$ ) (Hz)      | Second order frequency ( $f_2$ ) (Hz) | First order damping ratio ( $\xi_1$ ) | Second order damping ratio ( $\xi_2$ ) | First order frequency ( $f_1$ ) (Hz)      | Second order frequency ( $f_2$ ) (Hz) | First order damping ratio ( $\xi_1$ ) | Second order damping ratio ( $\xi_2$ ) | Fourier analysis (kPa)              | Wavelet analysis (kPa) |
| 1            | 20.5                                      | 58.6                                  | 0.085                                 | 0.029                                  | 29.4                                      | 60.4                                  | 0.027                                 | 0.018                                  | 101.3                               | 105.1                  |
| 2            | 30.0                                      | 59.25                                 | 0.071                                 | 0.0126                                 | 32.3                                      | 59.1                                  | 0.057                                 | 0.0188                                 |                                     |                        |
| 3            | 29.5                                      | 59.5                                  | 0.085                                 | 0.0126                                 | 33.1                                      | 59.0                                  | 0.07                                  | 0.036                                  |                                     |                        |
| 4            | 31.75                                     | 56.25                                 | 0.091                                 | 0.0088                                 | 32.1                                      | 57.8                                  | 0.082                                 | 0.0296                                 |                                     |                        |
| 5            | 32.0                                      | 57.0                                  | 0.090                                 | 0.0066                                 | 32.2                                      | 56.56                                 | 0.074                                 | 0.0248                                 |                                     |                        |

we filter the signal at 15–200 Hz, and then obtain the impulse response function of the system through random decrement technique [1], in which the width of data is 1000 points. The amplitude of the impulse response function is shown in Fig. 5b. We can see that it is difficult to read the plot directly because of the time limitation of the blow and burr of the plot. Therefore, it is necessary to identify the data through modal parameter identification methods.

The wavelet transform method is a simple and effective method and can be used for identifying the problem in which the difference between two adjacent modes is small. The other advantage of this method is that it can filter out the noise and thus it is not sensitive to the noise [5]. For these reasons, we use this method to analyze the experimental data.

We determine the frequency parameter of the discrete wavelet transform as  $\mathbf{a} = f_0/\mathbf{f}$ , where  $f_0 = \omega_0/(2\pi)$  is the modulated frequency, and  $\mathbf{f}$  is the frequency range vector of the structural system which is to be analyzed and is determined as  $\mathbf{f} = [20 : 0.2 : 80]$ . The wavelet transform of the experimental data has been made (see Fig. 6). We can determine the first two order natural frequency (see the center of the bright part of the plot), which are corresponding with the 60th and 198th point of the discrete frequency parameter. Based on the natural frequency, we choose frequency parameter  $a_1, a_2$  and identify the first two modal frequencies and damping ratio from Eqs. (6)–(9). The identifying results of the data in Table 3 are shown in Table 4. For making the problem clear, the phase of the wavelet transform of the second data set of Table 3 is shown in

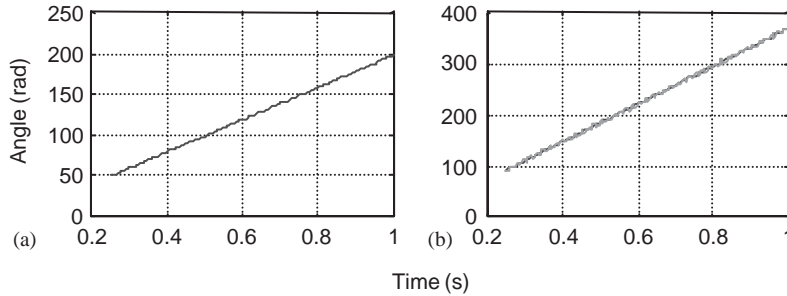


Fig. 7. Phase of the wavelet transform of the second data set of Table 3.

Fig. 7. The slopes of the lines in Figs. 7a and b are correspond with  $\omega_1\sqrt{1-\xi^2}$  and  $\omega_2\sqrt{1-\xi^2}$ , respectively. In Fig. 7, the real lines correspond with the results of identification and the dashed lines with the results of fitting.

Because the flutter of the missiles' wings is mainly coupled by warping and torsion of the first two modes, it is reasonable to use the flutter stability parameters method to predict the critical dynamic pressure. With this method, we can determine the flutter stability parameters by using the identifying results under the sub-critical state and the flutter characteristic equation of the two-degree-of-freedom system. The flutter stability parameters are as follows:

$$F = (A_2 - A_1/A_3)A_1 - A_0A_3 > 0, \tag{33}$$

where  $A_j$  ( $j = 0, 1, 2, 3$ ) are the parameters of the flutter characteristic equation of the two-degree-of-freedom system.  $F$  will vary with the experimental dynamic pressure of the wind tunnel. Its value reflects the extent of the stability of flutter. In the sub-critical state, the value of  $F$  is positive and decreases with the increase of dynamic pressure. Thus we can deduce the flutter critical dynamic pressure  $q_{cr}$  when  $F = 0$ . Usually, we use the following two order polynomial to fit the data:

$$B_0 + q_i B_1 + q_i^2 B_2 = F_i, \quad i = 1, 2, \dots, n, \tag{34}$$

where  $B_j$  ( $j = 0, 1, 2$ ) are the fitting parameters of the polynomial.  $q_i$  are the dynamic pressure of various sub-critical states.  $F_i$  are the corresponding flutter stability parameters. After getting the fitting parameters by using the least-squares fitting method, the critical dynamic pressure when  $F = 0$  can be predicted. Moreover, the modal parameters can be obtained through frequency response analysis that is done by a CF-920 FFT analyzer. The results are all shown in Table 4.

From Table 4, we can see that the difference between the values of the critical dynamic pressure predicted by Fourier analysis and wavelet analysis is small. The results of conventional Fourier analysis are smaller than those obtained by the wavelet method. So designing the structure of wings by using the critical dynamic pressure predicted by the Fourier analysis is somewhat conservative. However, they do not include the noise of wind tunnel, and there are many burrs in the real and imaginary part of the plot of the frequency response (see Fig. 8). Therefore, it would be difficult to analyze from these results and the error of identification would be great. On the contrary, although the wavelet transform method cannot eliminate the influence of noise, it is not sensitive to the noise. In general, the results of the wavelet transform method are calculated directly, not artificially found, so they would be more reliable.

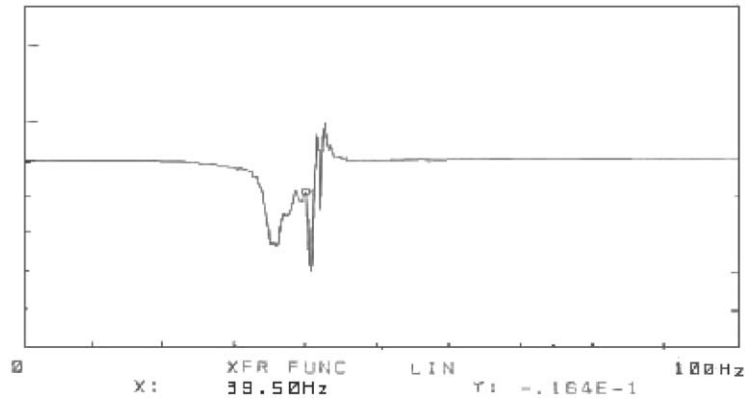


Fig. 8. Imaginary part of the frequency response function given by FFT analyzer.

Also in Table 4, we noted that there are many differences in the damping ratio between the two analyses. Usually, for a simple case, the difference should not be so large. But for a complex case like this, the question is different. In this case, the result got by FFT method may be influenced by two factors: the uncertainty of the inputted data caused by the noise in the wind tunnel and the error caused by artificially reading the data from Fig. 8. So we just used the FFT method as a reference.

## 8. Conclusions

The modal parameter identification method can make use of the modulated Gaussian wavelet transform based on the impulse response function. The Gaussian parameter can be used for modulating the accuracy of identification. This method is simple and effective. For the wind tunnel experiment of the wing model of missiles, when the dynamic pressure is increased gradually and the random decrease technique is used, the wavelet transform method is feasible, and more reliable and accurate results can be obtained.

## References

- [1] J.E. Cooper, Parameter estimation methods for flutter testing, AGARD, SMP Meeting, Rotterdam, May 1995.
- [2] W.J. Staszewski, J.E. Cooper, Flutter data analysis using the wavelet transform, Proceedings of the International Seminar on New Advances in Modal Synthesis of Large Structures: Nonlinear, Damped and Non-deterministic Cases, Lyon, France, 1995, pp. 203–214.
- [3] W.J. Staszewski, Identification of damping in MDOF systems using time-scale decomposition, Journal of Sound and Vibration 203 (2) (1997) 293–305.
- [4] M. Ruzzene, A. Fasana, L. Garibaldi, et al., Natural frequencies and dampings identification using wavelet transform: application to real data, Modern Solid State Physics 11 (2) (1997) 207–218.
- [5] C.H. Lamarque, S. Pernot, A. Cuer, Damping identification in multi-degree-of-freedom system via a wavelet-logarithmic decrement—part 1: theory, Journal of Sound and Vibration 235 (3) (2000) 361–374.